Applied Surface Science 715 (2026) 164586

Contents lists available at ScienceDirect

Applied Surface Science

journal homepage: www.elsevier.com/locate/apsusc

Full Length Article

Amine- and hydroxyl-functionalized copolymers as lubricant additives on Si-doped DLC: A comparative experimental and computational study of their tribological performance

Takeru Omiya [a,b,c,*], Enrico Pedretti [d], Manuel Evaristo [a], Pooja Sharma [a], Sara Inocencio [b], Albano Cavaleiro [a,c], Arménio C. Serra [b], Jorge F.J. Coelho [b,c], Maria Clelia Righi [d,**], Fábio Ferreira [a,c,*]

[a] University of Coimbra, CEMMPRE, ARISE, Department of Mechanical Engineering, Rua Luís Reis Santos, 3030-788 Coimbra, Portugal
[b] University of Coimbra, CEMMPRE, ARISE, Department of Chemical Engineering, Rua Silvio Lima, 3030-790 Coimbra, Portugal
[c] Laboratory for Wear, Testing & Materials, Instituto Pedro Nunes, Rua Pedro Nunes, 3030-199 Coimbra, Portugal
[d] Department of Physics and Astronomy, University of Bologna, Bologna 40127, Italy

ARTICLE INFO

Keywords:
Tribology
Functionalized copolymer
Diamond-like carbon
Temperature-dependent lubrication

ABSTRACT

Diamond-like carbon (DLC) coatings combined with functionalized copolymers are promising environmentally friendly lubrication systems and alternatives to metal containing additives. This study examines silicon-doped DLC (Si-DLC) lubricated with block copolymers bearing amine (DMAEMA) or hydroxyl (HEMA) groups. Friction and wear tests over 20–80 °C and under different loads show that both copolymers provide lower friction relative to nonfunctionalized PLMA, but only DMAEMA sustains low friction and low wear under 100 N boundary lubrication.

To clarify the mechanism, a distribution-based *ab initio* adsorption analysis was carried out on an amorphous Si-DLC model using a screening procedure across multiple surface sites and molecular orientations. The adsorption energy distributions show that DMAEMA frequently forms stable N–Si bonds (often ≤ -2.0 eV) and dual N–Si + O–Si bonds (about -2.4 eV), whereas HEMA centers near -1.5 eV for OH–Si bonds, with weaker dual OH–Si + O–Si bonding (about -2.0 eV). This separation of adsorption energy distributions accounts for the divergence in high load behavior.

Together, experiments and modeling underline the role of functional group chemistry in determining tribological performances on Si-DLC, and adsorption energy distributions, and guide additive selection for Si DLC in electric and hybrid drivetrains.

1. Introduction

Lubrication technology is rapidly evolving to meet the demands of higher fuel efficiency and the increasing adoption of electrified powertrains. Frictional losses still account for a significant portion of energy dissipation in vehicles, and in electric and hybrid vehicles, the operating environment differs from that of conventional engines [1,2]. Lower bulk-oil temperatures, more frequent start-stop cycles, and exposure to electrical currents require lubricants that are effective across a broad temperature range and under different mechanical and chemical conditions [3,4]. Lubricant additives are also at a pivotal stage of transformation, as the demand for environmentally benign and high-performance solutions continues to rise in parallel with shifts in engine technology and vehicle electrification. Zinc dialkyldithiophosphate (ZnDDP) has been a widely used anti-wear additive due to its ability to form protective films even under high-pressure conditions [5,6]. However, concerns about the sulfur and phosphorus content in ZnDDP, which can damage aftertreatment devices such as catalytic converters, have led to stricter regulations [7,8]. These environmental and regulatory challenges have accelerated the search for alternative additives that do not contain metals or ash-forming elements [9–11].

One promising alternative involves the use of functionalized block

* Corresponding authors at: University of Coimbra, CEMMPRE, ARISE, Department of Mechanical Engineering, Rua Luís Reis Santos, 3030-788 Coimbra, Portugal.
** Corresponding author at: Department of Physics and Astronomy, University of Bologna, Bologna 40127, Italy.
E-mail addresses: takeru.omiya@student.dem.uc.pt (T. Omiya), clelia.righi@unibo.it (M.C. Righi), fabio.ferreira@dem.uc.pt (F. Ferreira).

https://doi.org/10.1016/j.apsusc.2025.164586
Received 11 June 2025; Received in revised form 5 September 2025; Accepted 8 September 2025
Available online 9 September 2025

copolymers. These polymers contain nonpolar backbones for oil solubility and polar functional groups that can interact with surfaces. Early work demonstrated that methacrylate-based copolymers with carboxylic or amino groups can adsorb onto metallic surfaces and reduce friction under boundary conditions [12–14]. More recently, Kossoko et al. showed that a diblock PIB-PEG friction modifier (PFM) can achieve $\mu \approx 0.035$ at 100 °C by forming a chemisorbed polymer film on steel [15], while Gmür et al. used a nitrocatechol-grafted poly(lauryl methacrylate) brush to obtain 0.05 friction with only 0.5 wt% additive and confirmed nanometer-thick brush layers by QCM-D [16]. These results suggest that the surface interaction properties of the functional groups are more critical than the polymer backbone itself. However, such findings have been primarily demonstrated on conventional substrates such as steel, and comparative studies employing different functional groups on alternative tribological surfaces remain scarce.

In parallel, diamond-like carbon (DLC) coatings have been widely adopted in the automotive industry for their high hardness, excellent wear-resistance, chemical inertness and low friction [17–21]. The inherently low surface reactivity of DLC with conventional oils and additives, once considered a major limitation for achieving boundary lubrication in liquid lubrication systems [18,22], has been successfully addressed through elemental doping. As a result, a wide range of doped DLC coatings incorporating elements such as silicon has been developed to enhance interfacial interactions and tribochemical activity [23–26]. Omiya et al. demonstrated that combining silicon doped DLC (Si-DLC) with an amine-bearing block copolymer (PLMA-*b*-PDMAEMA) yields synergistic friction and wear reductions via the formation of strong N–Si interfacial bonds [27–29]. Nevertheless, it remains an open question whether other functional groups such as hydroxyl groups, which have been previously reported to reduce friction on steel [12,30,31], can offer comparable tribological benefits on Si-DLC surfaces, and whether their effectiveness is significantly influenced by operating temperature.

This study presents a comparative analysis of amine-functionalized (DMAEMA) and hydroxyl-functionalized (HEMA) block copolymers applied to an identical Si-DLC substrate over a broad temperature range (20–80 °C) and varying load conditions. A combined approach involving macro-scale tribometry and ab initio density functional theory is employed to elucidate the influence of anchor-group chemistry on adsorption energy and tribofilm stability. Temperature-dependent aggregation behavior, assessed by dynamic light scattering, is correlated with frictional performance to identify the operating regimes in which metal-free polymer/Si-DLC systems can fulfill the demanding low-temperature and high-load requirements of electric and hybrid vehicle drivetrains.

2. Materials and Methods

2.1. Coatings

The DLC coatings were deposited on M2 steel disks (50 mm diameter, 801 Vickers hardness), referring to previous studies [24]. The steel samples, polished to a surface roughness (Ra) of ~ 1 μm, underwent deposition in a Teer Coatings unbalanced magnetron sputtering system. This system employed four targets: pure chromium, pure graphite (two targets), and pure silicon. A 300 nm chromium interlayer was deposited first to enhance adhesion. The Si-DLC coating was approximately 1 μm thick. The coating composition was evaluated using SEM with EDS, and hardness and Young's modulus were measured using a Micromaterials Nanotest platform with a Berkovich indenter, applying a maximum load of 10 mN. Surface morphology was analyzed by AFM (Innova Veeco) in tapping modes with specific scan settings. The Si-DLC studied in this work contains 14.4 at.% Si and shows an average surface roughness (Ra) of 5.2 ± 0.2 nm. Its measured hardness reaches 19.4 ± 0.6 GPa, while the Young's modulus is 204 ± 4 GPa. The nanoindentation tests were carried out with a maximum load of 3 mN, and the resulting indentation depth did not exceed 10 % of the Si-DLC coating thickness (~1 μm). This ensured that the measured hardness and Young's modulus values reflect the intrinsic properties of the coating, minimizing the influence of the substrate. Further experimental details regarding the nanoindentation protocol can be found in our previous work [24,27]. XPS characterizations of samples prepared according to the same protocol were performed in our previous work [27,28], and indicate that the Si-DLC substrate is covered by a uniform Si-O-C mixed oxide layer with a thickness of about 1 nm. Previous Raman spectroscopy measurements on samples with the same Si concentration have shown that the formation of sp^3 bonds is promoted by the presence of Si, with an estimated sp^3 content of 56 % [27,28].

2.2. Lubricants

Copolymers of lauryl methacrylate (LMA) with 2-dimethylaminoethyl methacrylate (DMAEMA) (PLMA-*b*-PDMAEMA), as well as LMA with 2-hydroxyethyl methacrylate (HEMA) (PLMA-*b*-PHEMA), were synthesized via the Supplemental Activator and Reducing Agent Atom Transfer Radical Polymerisation (SARA ATRP) method (Fig. 1) [14]. In a typical procedure, copper wire (Cu0, 99.9 %: 1 mm diameter, 12 cm length) and copper (II) bromide (Acros Organics, 99 %: 0.015 mmol) were introduced into a Schlenk reactor under a nitrogen atmosphere. Separately, a mixture containing ethyl-α-bromophenylacetate (Sigma Aldrich, 97 %: 0.203 mmol), LMA, *N,N,N',N'',N''*-pentamethyldiethylenetriamine (Aldrich, 99 %: 0.045 mmol), and anisole (Sigma Aldrich, 99.0 %, 7.5 mL) was prepared and deoxygenated by purging with nitrogen. The Schlenk reactor was then immersed in a preheated oil bath to allow the polymerization of LMA to proceed for 3 h. For the synthesis of PLMA-*b*-PDMAEMA, DMAEMA (Acros Organics, 99 %: 7.81 mmol) was then added and the reaction was continued for another hour. To obtain PLMA-*b*-PHEMA, the same procedure was followed, except that after three hours of LMA polymerization, HEMA (TCI, 95 %: 4.93 mmol) was added instead of DMAEMA and stirring was continued for only 30 min. Both block copolymers were isolated using the same procedure [14] and their composition was determined by ^{1}H NMR (Table 1). The NMR chemical shift of the PLMA-*b*-PHEMA is shown in the Supplementary Information. The molecular weights and dispersity were measured using multi-detector calibration.

The lubricants were prepared from polyalphaolefin 4 (PAO 4) as the base lubricant with 8 wt% of the different polymers by mixing 8 g of the polymer in 92 g of PAO 4 using an analytical balance.

2.3. Tribological tests

To investigate friction behavior under low-load conditions, initial tribological tests were performed using a Rtec MFT-5000 tribometer (Rtec Instruments) in a reciprocating ball-on-disk setup. A 3/8-inch SiC ball was employed at a load of 3 N, corresponding to a Hertzian contact pressure of approximately 1.0 GPa. The stroke length was set to 15 mm, and testing was carried out for 20 min at a frequency of 0.2 Hz (sliding speed 0.006 m/s). The tribological tests were conducted under boundary lubrication conditions, as confirmed by a calculated λ value of 0.03 based on the Hamrock–Dowson equation [32]. In order to assess the polymer's temperature responsiveness, tests were conducted at 20 °C, 30 °C, 40 °C, 60 °C, and 80 °C, with the coefficient of friction recorded throughout. The temperature range of 20–80 °C was selected based on previous studies in which functionalized polymers exhibited significant friction-reducing effects around 80 °C [14,33]. In addition, this range reflects typical lubricant temperature conditions in hybrid and electric vehicles, where oil temperatures are generally lower than in conventional combustion engines and often remain below 80 °C during normal operation [3,4,34]. Thus, the selected range allows for the evaluation of both low- and high-temperature tribological behavior under conditions relevant to practical applications.

Subsequently, to evaluate wear performance under more severe (high-load) boundary lubrication conditions, an additional series of

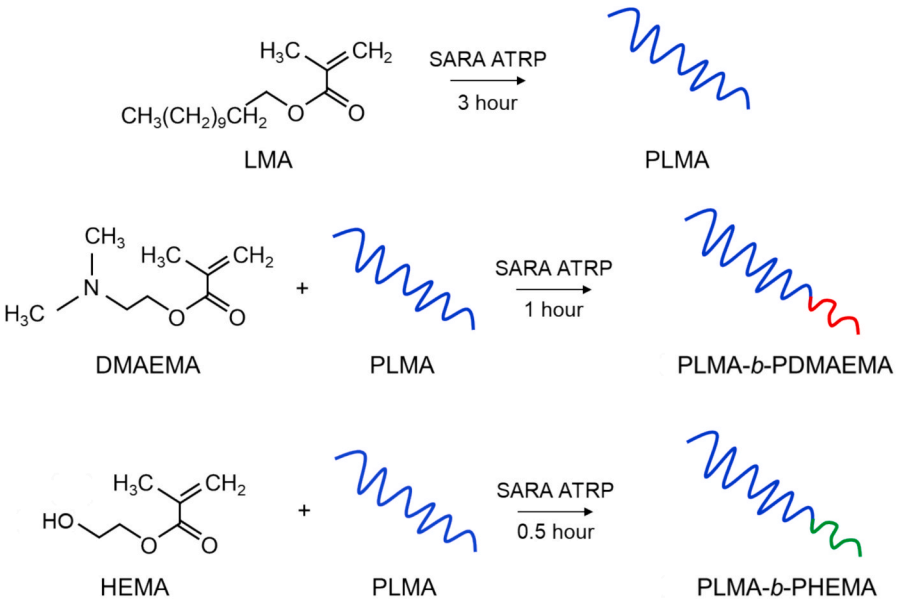

Fig. 1. Chemical structure of PLMA, PLMA-*b*-PDMAEMA and PLMA- *b* −PHEMA prepared by SARA ATRP.

Table 1
Physical properties of synthesized polymers.

Polymer Name	Ratio of each polymer [mol%]			M_w [kg/mol]	M_w/M_n
	PLMA	PDMAEMA	PHEMA		
PLMA	100	0	0	25	1.07
PLMA-*b*-PDMAEMA	90	10	0	26	1.06
PLMA-*b*-PHEMA	90	0	10	27	1.05

wear tests were performed using the same tribometer and SiC ball at 80 °C. In this case, the applied load was increased to 100 N, and the ball was reciprocated over a 1 mm stroke at 5 Hz for 20 min. After the tests, all samples were cleaned with heptane, and the wear scars were examined by white light interferometry (Rtec Instruments) to quantify wear volume. The reported wear rates represent mean values and standard deviations based on three repeated tests. By comparing the outcomes from these low- and high-load tests, the influence of load on both friction and wear performance was systematically assessed.

2.4. First principles calculations

Ab initio density functional theory (DFT) [35] calculations were performed to compare the adsorption energy of DMAEMA and HEMA functional groups on Si-DLC.

For the molecular adsorption study we employed our program Xsorb [36], that allows to screen a large number of initial adsorption configurations and efficiently identify the most relevant ones by employing a two-step optimization process. First, many initial structures are generated by combining translations (adsorption sites) and rotations of the molecule. In the pre-optimization step, all these initial structures are optimized with large convergence thresholds on energy and forces, in order to have an approximate outline of the distribution of adsorption energies, then a subset of the initial configurations are fully optimized with more stringent convergence thresholds (10^{-3} Ry/bohr on forces and 10^{-4} Ry on energies). In this case, we selected the subset for the full optimization by including the lowest energy configurations on a per-site basis, i.e. for a given site, we chose a subset of among the molecular rotations that resulted in lower energy in the pre-optimization stage.

The structures of the DMAEMA and HEMA monomers are shown in Fig. 2a and Fig. 2b, respectively. For both molecules, the hydrocarbon chain was terminated with methyl groups on the two sides where the

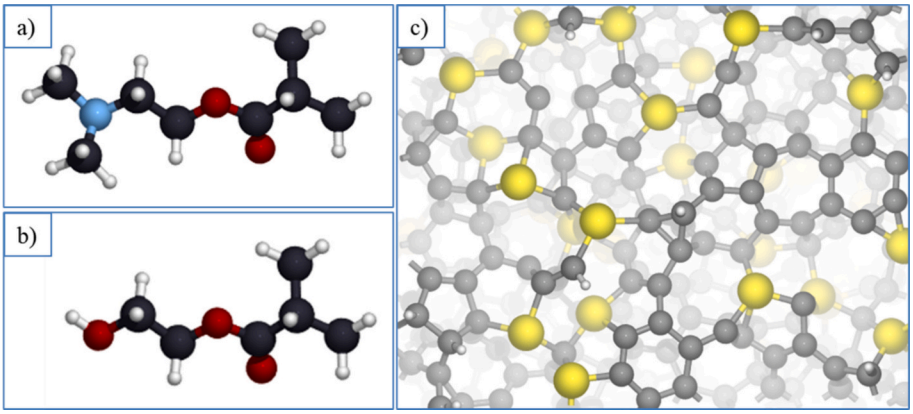

Fig. 2. Ball and stick representation of the DMAEMA (a) and HEMA (b) functional groups, and top view of the Si-doped DLC surface model (c). Highly reactive undercoordinated C atoms in the Si-DLC surface were passivated with H atoms. In the images, C atoms are colored in black (molecules) and grey (surface), H atoms are colored in white, O in red, N in blue and Si in yellow.

monomer is connected to the repeating units to form the polymer. For the Si-DLC, an amorphous model with 10 at.% Si concentration was generated with melt-quench molecular dynamics simulations, using the pre-trained universal machine learning force field CHGNet [37]. The radial pair distribution function, bond angle distribution and coordination number were checked to validate the model. The bulk amorphous structure was then cut to obtain a slab, annealed with molecular dynamics to heal the surface dangling bonds, and optimized with DFT. A few H atoms were added to passivate some remaining very reactive, under-coordinated carbon atoms, finally obtaining the surface visible in Fig. 2c.

For the molecular adsorption study with Xsorb, we generated many initial adsorption configurations by placing the functional groups of each monomer on superficial Si atoms (adsorption sites) of Si-DLC. As functional groups we considered the (tertiary) amine group for DMAEMA and the hydroxyl group for HEMA, corresponding to the actual "active region" of the two molecules, and also the carbonyl group (part of the ester group) which is common to both molecules. Regarding molecular rotations, it was not possible to choose meaningful rotation angles from the symmetries of the surface due to its amorphous nature, and a reasonable tradeoff between computational cost and sampling coverage was obtained by including 4 horizontal molecular rotations of multiples of 90° for each site. The combination of 4 rotations per site and 8 surface sites resulted in 72 initial adsorption configurations for each molecule. For each site, the most favorable adsorption configuration in the pre-optimization step (out of the 4 corresponding to the rotations for that site) was selected for the full optimization, resulting in 16 fully optimized adsorption structures for each molecules that were considered for the analysis of the adsorption energy distribution.

All the (spin-polarized) DFT calculations were performed with the plane wave code implemented in Quantum Espresso [38], using the Perdew-Burke-Ernzerhof (PBE) parametrization [39] of the generalized gradient approximation (GGA) for the exchange–correlation functional. The core electrons were approximated by employing ultrasoft pseudopotentials [40] and van der Waals dispersion interactions were included with the semi-empirical Grimme D2 [41] scheme. The plane wave expansion was truncated at a kinetic energy cutoff of 40 Ry for the wavefunctions and 320 Ry for the charge density.

The lateral size of the Si-DLC simulation cells was 18.8 Å × 15.0 Å, with a slab thickness of ~ 10 Å, and a vacuum region of 14 Å in the z-direction to suppress interactions with the periodic replicas (leaving approximately 10 Å of vacuum with the molecule adsorbed on the surface). Due to the large size of the cell, the Brillouin zone was sampled only at the Γ-point.

2.5. Dynamic light scattering

Dynamic light scattering (DLS) measurements were performed to evaluate the size distribution of polymer aggregates in PAO 4 at different temperatures. The aim of the analysis was to determine the temperature-dependent structural states of the synthesized copolymers (PLMA, PLMA-*b*-PDMAEMA, and PLMA-*b*-PHEMA) and their impact on lubrication performance. DLS measurements were performed using a Malvern Zetasizer Nano ZS instrument equipped with a He-Ne laser (633 nm, 4 mW) at a scattering angle of 173°. Samples were prepared by dissolving each polymer in PAO 4 at a concentration of 8 wt%, followed by stirring at 60 °C for 1 h to ensure homogeneous dispersion. The particle size distribution was measured at four different temperatures: 20 °C, 40 °C, 60 °C, and 80 °C.

3. Results and Discussion

3.1. Friction test in Low-Load Condition

To assess the tribological performance of PLMA, PLMA-*b*-PDMAEMA, and PLMA-*b*-PHEMA, friction tests were conducted at five different temperatures (20 °C, 30 °C, 40 °C, 60 °C, and 80 °C), as illustrated in Fig. 3. In all tested temperatures, the functionalized copolymers (PLMA-*b*-PDMAEMA and PLMA-*b*-PHEMA) consistently exhibited lower friction coefficients than PLMA. This observation is consistent with previous findings, where the amino groups in PLMA-*b*-PDMAEMA interacted strongly with silicon-containing surfaces to form tribofilms [27]. By analogy, the hydroxyl groups in PLMA-*b*-PHEMA are similarly inferred to interact with the silicon in Si-DLC, promoting friction reduction.

A clear temperature dependence was also found. Friction generally decreased with increasing temperature. For PLMA, friction initially decreased at 60 °C and 80 °C, but began to increase after about five minutes of testing. In contrast, the functionalized copolymers showed a rapid decrease in friction from 40 °C and remained in a stable low-friction state until the end of the tests. This behavior suggests that the functional groups in these copolymers enable robust adsorption on the Si-DLC surface and maintain effective lubrication even at higher temperatures.

At the lower temperatures of 20 °C and 30 °C, it took longer for the

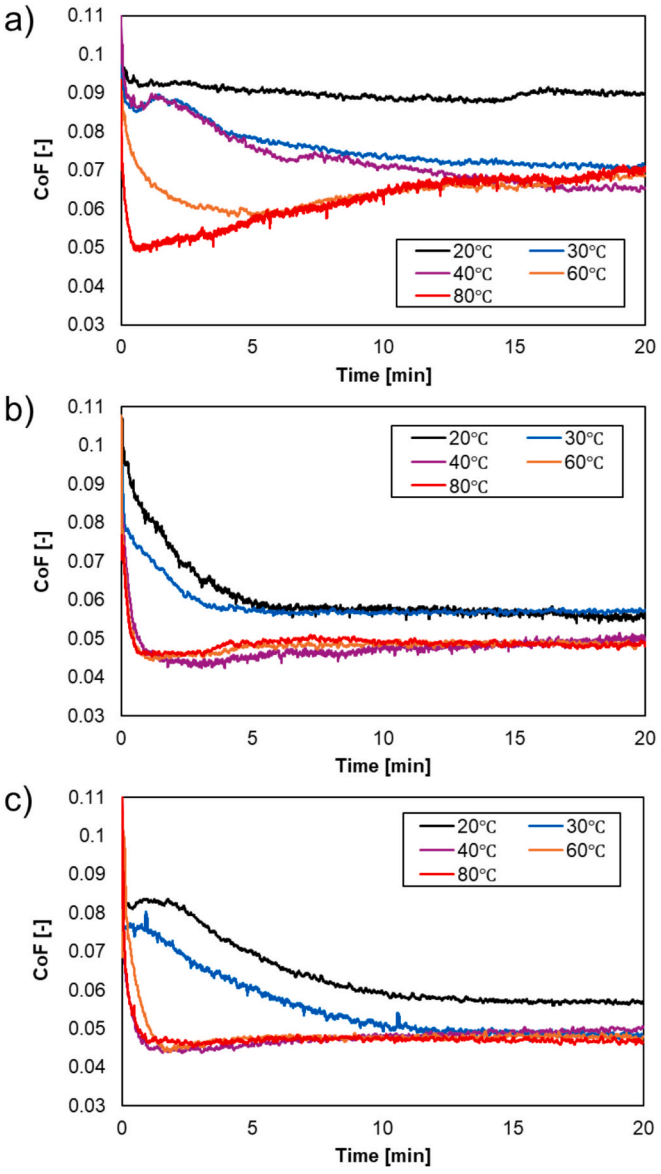

Fig. 3. Friction coefficient evolution of (a) PLMA, (b) PLMA-*b*-PDMAEMA, and (c) PLMA-*b*-PHEMA as a function of time at different temperatures on Si-DLC surfaces.

functionalized copolymers to stabilize in a low-friction regime. This delay can be attributed to the temperature-dependent structural states of the polymers, which influence how quickly the copolymers adsorb to the surface. This explanation is also supported by the accompanying DLS analyses. In addition, PLMA-*b*-PDMAEMA showed a sharper initial reduction in friction at these temperatures compared to PLMA-*b*-PHEMA. This suggests possible differences in the interactions of the functional groups of PLMA-*b*-PDMAEMA and PLMA-*b*-PHEMA with the Si-DLC surface.

3.2. Wear test in High-Load Condition

The wear performance was then evaluated for each of the three polymer solutions. Fig. 4(a) shows the average coefficient of friction measured one minute before the completion of the friction test, while Fig. 4(b) compares the wear ratio between the samples. PLMA-*b*-PDMAEMA exhibited the lowest coefficient of friction and the wear ratio. Although PLMA-*b*-PHEMA had a reduced wear ratio compared to PLMA, its coefficient of friction remained at a similar level to that of PLMA. In line with the results of friction tests, these results confirm that PLMA-*b*-PDMAEMA performs better than PLMA-*b*-PHEMA in terms of both friction and wear. The evolution of the friction coefficient over the entire 20-minute duration is presented in **Fig. S2** of the Supplementary Information.

3.3. First principles molecular adsorption calculations

Our previous studies have shown that the adsorption of DMAEMA functional groups on the Si-DLC surface is a key factor for the formation of a stable lubricating film that can reduce friction and wear even under harsh conditions of boundary lubrication [27]. By forming strong N-Si bonds, the adsorbed functional groups act as anchoring points for the entire copolymer, forming a lubricating film that can withstand the extreme mechanical forces that occur at surface asperities and prevent the additives from being expelled from the contacts under high loads, reducing the risk of adhesion to the counter-surface. Through a comparative *ab initio* analysis of the adsorption of DMAEMA and HEMA, we aim to evaluate the ability of HEMA to form bonds with the Si-DLC surface via the hydroxyl group, compared to the analogous mechanism of DMAEMA via the amine group.

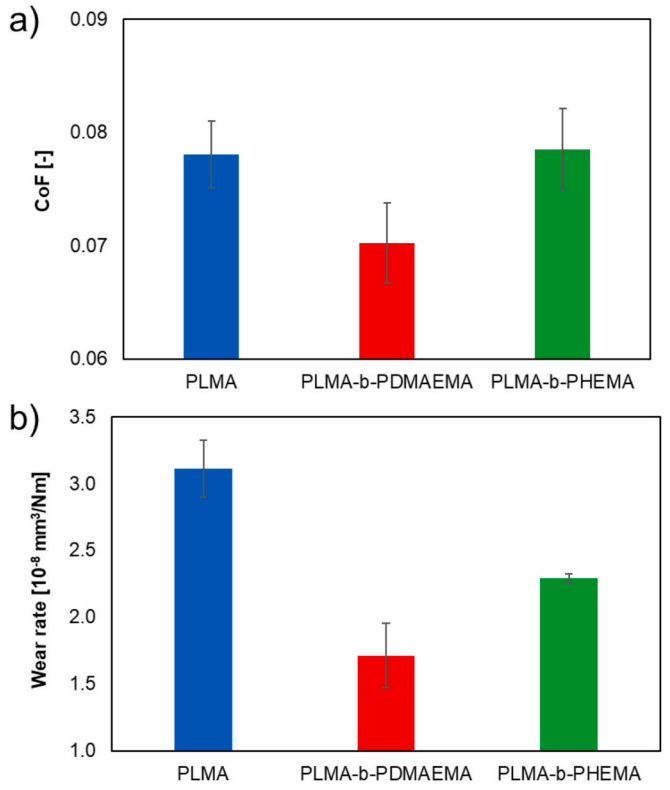

Fig. 4. (a) Average friction coefficient measured one minute before test completion, and (b) comparison of wear ratios for PLMA, PLMA-*b*-PDMAEMA, and PLMA-*b*-PHEMA.

Due to the random nature of the amorphous Si-DLC, we investigated the adsorption processes from a statistical point of view. Using the Xsorb program, we generated many initial adsorption configurations, considering adsorption on different Si atoms on the surface and different orientations of the molecule. A two-step screening process was applied, consisting of an initial partial optimization of all the generated structures, and a final full optimization of the most relevant configuration for each adsorption site. A more detailed explanation of the procedure can be found in the Methods section.

For each molecule, 72 initial configurations were tested in the pre-optimization stage, of which 16 were fully optimized and considered for the energy distribution analysis. Representatives of the different bonding modes for DMAEMA and HEMA are reported in Fig. 5a and Fig. 5c, respectively. Both molecules show analogous bonding patterns with Si atoms of the surface: through the functional "head" group (tertiary amine for DMAEMA and hydroxyl for HEMA), through the carbonyl group, or both at the same time. For comparison, weakly physisorbed configurations are included for the two molecules. The distribution of adsorption energies for DMAEMA and HEMA are reported in the histograms of Fig. 5b and Fig. 5d, with color coding representing the different bonds described above. The adsorption energy is defined as

$$E_{ads} = E_{slab+mol} - E_{slab} - E_{mol}$$

where $E_{slab+mol}$ is the energy of the structure with the molecule adsorbed on the slab, E_{slab} is the energy of the slab without the molecule, and E_{mol} is the energy of the molecule in vacuum. Using this definition, more negative values of adsorption energy correspond to more favorable adsorption.

The distribution of adsorption energies clearly shows that HEMA is less strongly adsorbed than DMAEMA: bonds formed by the OH group of HEMA are associated with an adsorption energy of −1.5 eV (green peak in Fig. 5d), while N-Si bonds of DMAEMA are below −2 eV (blue bar in Fig. 5b). The same trend is observed for the configuration with two bonds, involving also the carbonyl group: OH-Si + O-Si results in an adsorption energy of −2 eV for HEMA, while N-Si + O-Si reaches −2.4 eV for DMAEMA. By taking as reference the energy of weak physisorption (generally larger than −1 eV for both molecules), the N-Si bond in DMAEMA is significantly stronger (more than 1 eV energy gain with respect to physisorption) than the OH-Si bond in HEMA (0.5 eV energy gain).

These computational results agree very well with the experimental observations: at low loads, both DMAEMA and HEMA show good tribological performances, with a similar reduction of CoF. This can be attributed to the fact that the functional groups allow the formation of chemical bonds with Si-DLC, anchoring the whole copolymers and forming an adsorbed lubricating film. On the other hand, under more extreme conditions of high load, only DMAEMA is able to maintain good tribological performances (friction and wear reduction) as it is able to form much more stable bonds, while the weaker bonds of HEMA can be broken by such strong mechanical forces and the copolymer film is more likely to detach from the surface.

While the computational study is limited to monomers rather than the full polymer chains, the main goal is to compare the local strength of the bonds that can be formed between the functional groups of the two molecules. Furthermore, due to the low amount of available Si atoms at the surface (10 % doping), the effect of nearby monomers is not likely to strongly affect the adsorption mechanism (e.g. through the formation of

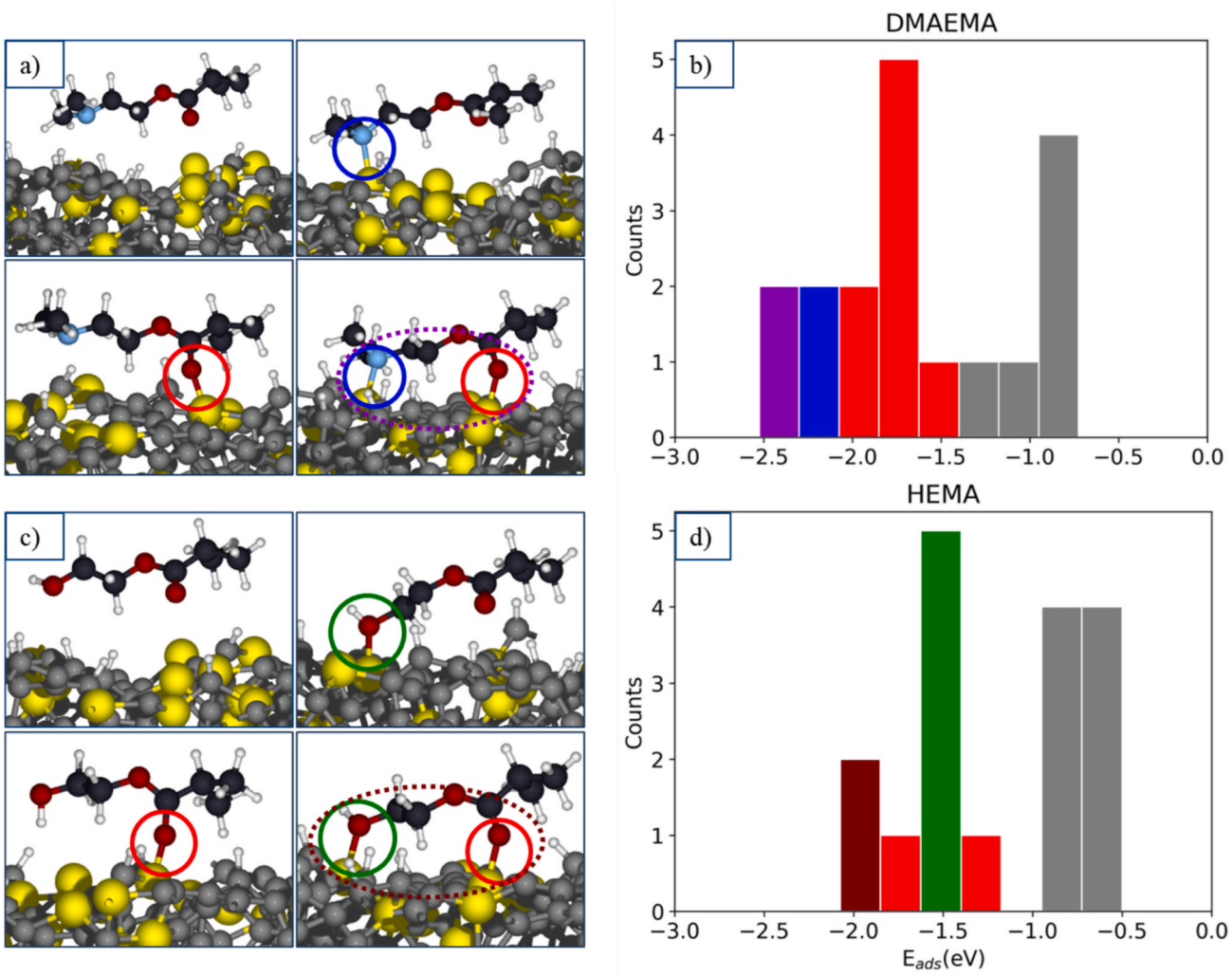

Fig. 5. Representative configurations of the four bonding modes for DMAEMA (a) and HEMA (c) on Si-DLC: weak physisorption (no bonding), bonding through the functional "head" group (tertiary amine for DMAEMA – N-Si bond circled in blue – and hydroxyl for HEMA – OH-Si bond circled in green), through the carbonyl group (O-Si bond – circled in red), or both at the same time. C atoms are colored in black (molecules) and grey (surface), H atoms are colored in white, O in red, N in blue and Si in yellow. (b), (d): histograms of the adsorption energy distribution for DMAEMA and HEMA, using the same color code as the bonds in (a,c), and grey bars for physisorption. Configurations with two bonds are colored in purple (DMAEMA) and brown (HEMA), as the dashed ellipses in (a,c).

a self-assembled monolayer with lateral van der Waals interactions between the monomers, which would require a much higher density of surface Si dopants).

From this analysis it appears that under mild, low load conditions the OH group in HEMA is able to reduce friction by chemically bonding to the Si atoms in Si-DLC, analogous to DMAEMA, while under harsher, high load conditions the OH-Si bond is not strong enough to maintain the anchoring of the adsorbed film to the surface, so HEMA cannot provide friction and wear reduction.

3.4. *Particle size evaluation using DLS*

In order to determine the temperature-dependent structural states of the polymers, DLS measurements were carried out at four different temperatures: 20 °C, 40 °C, 60 °C, and 80 °C. Fig. 6 shows the particle sizes observed for the three polymers in PAO solutions under these conditions. A clear trend can be seen, where the measured particle size decreases with increasing temperature. In general, many oil-based viscosity index improvers exhibit relatively collapsed chains at lower temperatures. At higher temperatures, their affinity for oil improves, resulting in enhanced solubility and an expanded coil volume. In this study, the polymers had a molecular weight of about 25 kg/mol, and the

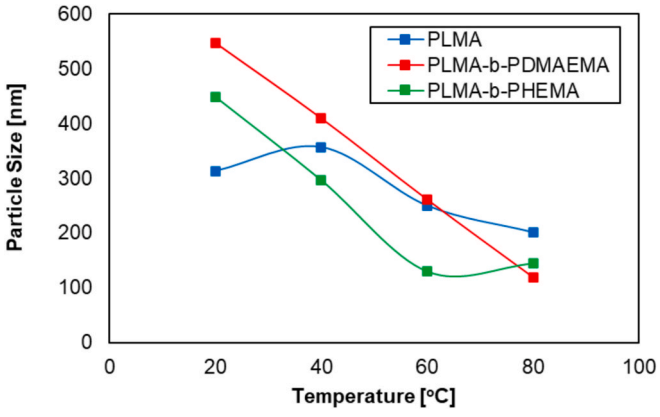

Fig. 6. DLS-measured particle sizes of PLMA, PLMA-*b*-PDMAEMA, and PLMA-*b*-PHEMA at 20 °C, 40 °C, 60 °C, and 80 °C.

chain length was estimated to be a few tens of nanometers. The structures detected by DLS, which were several hundred nanometers in size, indicate that these measurements are polymer aggregates rather than

individual polymer chains. This suggests that the aggregates formed at lower temperatures gradually disintegrate as the temperature increases.

A particularly interesting observation is that the functionalized copolymers at 20 °C have significantly larger aggregates of about 500 nm compared to PLMA. This suggests that the functional groups present in the copolymers promote micelle-like assemblies, leading to larger aggregates compared to non-functionalized PLMA. The results of the friction test support this interpretation. At 20 °C, the functionalized copolymers showed less pronounced friction reduction. The DLS results indicate that the large aggregates probably hinder the adsorption of the functional groups on the surface, and thus reduce the effectiveness of friction reduction. On the other hand, the aggregates gradually disintegrated at higher temperatures. This facilitated the migration of the functional groups to the surface and contributed to improved friction reduction and wear performance.

4. Conclusion

In this study, we investigated the tribological behavior of Si-DLC coatings lubricated with oil-soluble block copolymers bearing amine (PLMA-*b*-PDMAEMA) or hydroxyl (PLMA-*b*-PHEMA) functional groups, complemented by experimental and first-principles analyses. Tribological tests showed that both functionalized copolymers significantly reduce friction compared to non-functionalized PLMA, particularly at higher temperatures. DLS measurements showed that the functionalized copolymers formed larger polymer aggregates at lower temperatures, which slowed adsorption on the surface and delayed friction reduction. At higher temperatures, the degradation of these aggregates promoted rapid surface adsorption and improved lubricity.

First-principles DFT calculations showed that the amine-containing DMAEMA units formed more stable N–Si bonds with Si-DLC than the hydroxyl-containing HEMA units, resulting in lower adsorption energies (more negative) and stronger surface anchoring. This theoretical finding is consistent and can explain the experimental observation that PLMA-*b*-PDMAEMA exhibits better frictional and wear performance than PLMA-*b*-PHEMA. Although both amine and hydroxyl groups reduce friction under mild conditions, only the stronger amine–Si bond can withstand the high contact stresses typically encountered in boundary lubrication. These results are clear evidence that optimizing the functional groups of the copolymer to build robust interfacial bonds with Si-DLC is crucial for sustained friction and wear reduction. Furthermore, the temperature-dependent structural states of the polymeric additives, as revealed by DLS, illustrate the importance of controlling aggregate behavior to ensure rapid surface adsorption and effective lubrication. Overall, this work provides valuable insight into the development of advanced lubricant additives that combine targeted surface chemistry with favorable thermal behavior to enable improved tribological performance under a wide range of operating conditions.

CRediT authorship contribution statement

Takeru Omiya: Writing – original draft, Visualization, Validation, Software, Project administration, Methodology, Investigation, Formal analysis, Data curation, Conceptualization. **Enrico Pedretti:** Writing – review & editing, Visualization, Validation, Software, Methodology, Investigation, Formal analysis, Data curation. **Manuel Evaristo:** Investigation. **Pooja Sharma:** Writing – review & editing, Investigation, Data curation. **Sara Inocencio:** Formal analysis, Data curation. **Albano Cavaleiro:** Writing – review & editing, Supervision, Resources, Funding acquisition. **Arménio C. Serra:** Writing – review & editing, Resources, Funding acquisition. **Jorge F.J. Coelho:** Writing – review & editing, Supervision, Project administration, Funding acquisition, Conceptualization. **Maria Clelia Righi:** Writing – review & editing, Supervision, Resources, Project administration, Funding acquisition, Conceptualization. **Fábio Ferreira:** Writing – review & editing, Supervision, Resources, Funding acquisition, Conceptualization.

Declaration of competing interest

The authors declare that they have no known competing financial interests or personal relationships that could have appeared to influence the work reported in this paper.

Acknowledgments

This research is sponsored by national funds through FCT – Fundação para a Ciência e a Tecnologia, under the project UIDB/00285/2020, LA/P/0112/2020, 2023.08138.CEECIND/CP2832/CT0005, SmartHyLub (2022.05603.PTDC), iLub (2022.15609.UTA), UniLub (2023.17357.ICDT) and by the Taiho Kogyo Tribology Research Foundation (Grant No. 22A25). This project has received funding from the European Union's Horizon 2020 research and innovation programme under grant agreement No 101007417, having benefited from the access provided by the Karlsruhe Institute of Technology within the framework of the NFFA-Europe Pilot Transnational Access Activity, proposal ID580.

These results are part of the "Advancing Solid Interface and Lubricants by First Principles Material Design (SLIDE)" project that has received funding from the European Research Council (ERC) under the European Union's Horizon 2020 research and innovation program (Grant agreement No. 865633).

Appendix A. Supplementary data

Supplementary data to this article can be found online at https://doi.org/10.1016/j.apsusc.2025.164586.

Data availability

Data will be made available on request.

References

[1] K. Holmberg, P. Andersson, N.-O. Nylund, K. Mäkelä, A. Erdemir, Global energy consumption due to friction in trucks and buses, Tribol. Int. 78 (2014) 94–114.
[2] Y. Huang, N.C. Surawski, B. Organ, J.L. Zhou, O.H. Tang, E.F. Chan, Fuel consumption and emissions performance under real driving: Comparison between hybrid and conventional vehicles, Sci. Total Environ. 659 (2019) 275–282.
[3] T. Yuksel, J.J. Michalek, Effects of regional temperature on electric vehicle efficiency, range, and emissions in the United States, Environ. Sci. Technol. 49 (2015) 3974–3980.
[4] H. Jikuya, S. Mori, K. Yamamori, S. Hirano, Development of firing fuel economy engine dyno test procedure for JASO ultra low viscosity engine oil standard (JASO GLV-1), SAE Technical Paper (2019).
[5] P. Willermet, D. Dailey, R. Carter Iii, P. Schmitz, W. Zhu, Mechanism of formation of antiwear films from zinc dialkyldithiophosphates, Tribol. Int. 28 (1995) 177–187.
[6] M.A. Nicholls, T. Do, P.R. Norton, M. Kasrai, G.M. Bancroft, Review of the lubrication of metallic surfaces by zinc dialkyl-dithiophosphates, Tribol. Int. 38 (2005) 15–39.
[7] A. Sappok, R. Rodriguez, V. Wong, Characteristics and effects of lubricant additive chemistry on ash properties impacting diesel particulate filter service life, SAE Int. J. Fuels Lubr. 3 (2010) 705–722.
[8] M.M. Maricq, R.E. Chase, N. Xu, D.H. Podsiadlik, The effects of the catalytic converter and fuel sulfur level on motor vehicle particulate matter emissions: gasoline vehicles, Environ. Sci. Technol. 36 (2002) 276–282.
[9] B. Kim, R. Mourhatch, P.B. Aswath, Properties of tribofilms formed with ashless dithiophosphate and zinc dialkyl dithiophosphate under extreme pressure conditions, Wear 268 (2010) 579–591.
[10] B. Kim, J.C. Jiang, P.B. Aswath, Mechanism of wear at extreme load and boundary conditions with ashless anti-wear additives: Analysis of wear surfaces and wear debris, Wear 270 (2011) 181–194.
[11] J. Qu, H. Luo, M. Chi, C. Ma, P.J. Blau, S. Dai, et al., Comparison of an oil-miscible ionic liquid and ZDDP as a lubricant anti-wear additive, Tribol. Int. 71 (2014) 88–97.
[12] M. Muller, K. Topolovec-Miklozic, A. Dardin, H.A. Spikes, The design of boundary film-forming PMA viscosity modifiers, Tribol. Trans. 49 (2006) 225–232.
[13] J. Fan, M. Müller, T. Stöhr, H.A. Spikes, Reduction of Friction by Functionalised Viscosity Index Improvers, Tribol. Lett. 28 (2007) 287–298.
[14] T. Omiya, F. De Bon, T. Vuchkov, A. Serra, A. Cavaleiro, J. Coelho, et al., Wear resistance by copolymers with controlled structure under boundary lubrication conditions, Lubr. Sci. 36 (2024) 1–8.

[15] N.F. Kossoko, F. Dubreuil, B. Thiébaut, M. Belin, C. Minfray, Diblock polymeric friction modifier (PFM) in the boundary regime: Tribological conditions leading to low friction, Tribol. Int. 163 (2021) 107186.
[16] T.A. Gmür, J. Mandal, J. Cayer-Barrioz, N.D. Spencer, Towards a Polymer-Brush-based friction modifier for oil, Tribol. Lett. 69 (2021) 124.
[17] A. Erdemir, C. Donnet, Tribology of diamond-like carbon films: recent progress and future prospects, J. Phys. D Appl. Phys. 39 (2006) R311.
[18] B. Podgornik, J. Vižintin, Tribological reactions between oil additives and DLC coatings for automotive applications, Surf. Coat. Technol. 200 (2005) 1982–1989.
[19] R. Cruz, J. Rao, T. Rose, K. Lawson, J.R. Nicholls, DLC–ceramic multilayers for automotive applications, Diam. Relat. Mater. 15 (2006) 2055–2060.
[20] M. Kano, Diamond-like Carbon Coating Applied to Automotive Engine Components, Tribology Online. 9 (2014) 135–142.
[21] Z.-y. Xing, J.-y. Zhang, R. Kaindl, B. Zhang, Solid superlubricity of diamond-like carbon films: a review, Surface Science and Technology. 3 (2025) 16.
[22] M. Kalin, I. Velkavrh, J. Vižintin, L. Ožbolt, Review of boundary lubrication mechanisms of DLC coatings used in mechanical applications, Meccanica 43 (2008) 623–637.
[23] G. Ma, S. Gong, G. Lin, L. Zhang, G. Sun, A study of structure and properties of Ti-doped DLC film by reactive magnetron sputtering with ion implantation, Appl. Surf. Sci. 258 (2012) 3045–3050.
[24] M. Evaristo, R. Azevedo, C. Palacio, A. Cavaleiro, Influence of the silicon and oxygen content on the properties of non-hydrogenated amorphous carbon coatings, Diam. Relat. Mater. 70 (2016) 201–210.
[25] R. Zahid, M.B.H. Hassan, A. Alabdulkarem, M. Varman, R.A. Mufti, M.A. Kalam, et al., Investigation of the tribochemical interactions of a tungsten-doped diamond-like carbon coating (W-DLC) with formulated palm trimethylolpropane ester (TMP) and polyalphaolefin (PAO), RSC Adv. 7 (2017) 26513–26531.
[26] T. Omiya, A. Cavaleiro, N. Figueiredo, R. Gouttebaron, A. Felten, F. Ferreira, Sustainable Lubrication through Gd DLC Films and Ionic Liquids for Wear and Corrosion Resistance, Tribol. Int. 110130 (2024).
[27] T. Omiya, E. Pedretti, M. Evaristo, A. Cavaleiro, A.C. Serra, J.F. Coelho, et al., Synergistic effects of nitrogen-containing functionalized copolymer and silicon-doped DLC for friction and wear reduction, Tribol. Int. 200 (2024) 110183.
[28] T. Omiya, E. Pedretti, A. Cavaleiro, R. Gouttebaron, A. Felten, A.C. Serra, et al., Elucidating the composition and formation mechanism of slippery films from block copolymers on doped diamond-like carbon surfaces, Appl. Surf. Sci. 163599 (2025).
[29] T. Omiya, A. Welle, M. Evaristo, P. Sharma, A. Cavaleiro, A.C. Serra, et al., Polymer derived tribofilm on silicon-doped diamond-like carbon coatings, Appl. Surf. Sci. 164200 (2025).
[30] L. Bostan, A.-M. Trunfio-Sfarghiu, L. Verestiuc, M. Popa, F. Munteanu, J.-P. Rieu, et al., Mechanical and tribological properties of poly (hydroxyethyl methacrylate) hydrogels as articular cartilage substitutes, Tribol. Int. 46 (2012) 215–224.
[31] K. Şarkaya, G. Akıncıoğlu, S. Akıncıoğlu, Investigation of tribological properties of HEMA-based cryogels as potential articular cartilage biomaterials, Polym.-Plast. Technol. Mater. 61 (2022) 1174–1190.
[32] B.J. Hamrock, D. Dowson, Ball Bearing Lubrication (the Elastohydrodynamics of Elliptical Contacts), J. Lubr. Technol. 104 (1981) 279–281.
[33] M. Müller, K. Topolovec-Miklozic, A. Dardin, H.A. Spikes, The design of boundary film-forming PMA viscosity modifiers, Tribol. Trans. 49 (2006) 225–232.
[34] B. Leach, R. Pearson, Engine Lubrication and Cooling during Hybrid Vehicle operation, SAE Technical Paper (2014).
[35] P. Hohenberg, W. Kohn, Inhomogeneous Electron Gas. Physical Review. 136 (1964) B864.
[36] E. Pedretti, P. Restuccia, M.C. Righi, Xsorb: a software for identifying the most stable adsorption configuration and energy of a molecule on a crystal surface, Comput. Phys. Commun. 291 (2023) 108827.
[37] B. Deng, P. Zhong, K. Jun, J. Riebesell, K. Han, C.J. Bartel, et al., CHGNet as a pretrained universal neural network potential for charge-informed atomistic modelling, Nat. Mach. Intell. 5 (2023) 1031–1041.
[38] P. Giannozzi, S. Baroni, N. Bonini, M. Calandra, R. Car, C. Cavazzoni, et al., QUANTUM ESPRESSO: a modular and open-source software project for quantum simulations of materials, J. Phys. Condens. Matter 21 (2009) 395502.
[39] J.P. Perdew, K. Burke, M. Ernzerhof, Generalized gradient approximation made simple, Phys. Rev. Lett. 77 (1996) 3865.
[40] D. Vanderbilt, Soft self-consistent pseudopotentials in a generalized eigenvalue formalism, Phys. Rev. B 41 (1990) 7892.
[41] S. Grimme, Semiempirical GGA-type density functional constructed with a long-range dispersion correction, J. Comput. Chem. 27 (2006) 1787–1799.